Journal of Structural Geology, Vol. 14, No. 3, pp. 315 to 321, 1992
Printed in Great Britain

0191-8141/92 $05.00+0.00

The origin of ridge-in-groove slickenside striae and associated steps in an *S–C* mylonite

SHOUFA LIN and PAUL F. WILLIAMS

Department of Geology, University of New Brunswick, Fredericton, N.B., Canada E3B 5A3

(*Received* 4 *December* 1990; *accepted in revised form* 12 *July* 1991)

Abstract—A three-dimensional study of an *S–C* mylonite reveals that the *S*-surfaces anastomose around porphyro-clasts and *C*-surfaces are not truly planar, but curvi-planar with the linear generator parallel to the movement direction. It is suggested that it may be common for shear surfaces at all scales to take this form. In the material studied, surfaces exposed by parting primarily along *C*-surfaces, which are a product of ductile deformation and are penetrative, have all the characteristics of classic slickensides. On the slickensides, striae of the 'ridge-in-groove' type and steps of both congruous and incongruous types are developed. The 'ridge-in-groove' shape of the striae is directly related to the curvi-planar shape of the *C*-surfaces. Incongruous steps are smooth. They are the result of parting along *S*-surfaces. Congruous steps are rough. First-order congruous steps are formed by fracturing between individual *C*-surfaces, whereas second-order congruous steps form by breaking off the tips of the dihedra between *S*- and *C*-surfaces. Thus, the 'smoothness–roughness' technique can be used to determine the sense of shear. In strongly deformed rocks, where the angle between *S*- and *C*-surfaces is too small to be recognized in the field, this may prove to be a useful shear sense indicator.

INTRODUCTION

CLASSICAL slickensides are smooth or shiny, commonly striated shear surfaces in rocks (e.g. Fleuty 1975). They are widely believed to result from brittle deformation (e.g. Bates & Jackson 1987). However, recent observations have shown that this may not always be true. Slickensides (or slickenside striations) have been found in ductilely deformed rocks (Berthé *et al.* 1979, Burg & Ponce de Leon 1985, Burg & Wilson 1988, and this study), and Will & Wilson (1989) interpreted the experimentally produced 'ridge-in-groove'-type slickenside striation of Means (1987) as a product of ductile deformation.

Here we describe natural slickensides developed in an *S–C* mylonite. These slickensides have the classic appearance, but are genetically related to the penetrative *S–C* structure. We confirm that the 'ridge-in-groove'-type slickenside striation can form during ductile deformation, and also demonstrate that slickenside steps can be associated with the same *S–C* structure.

The *S–C* mylonite is developed in the Black Brook granite, in the Eastern Highlands shear zone on Cape Breton Island, Nova Scotia, Canada (Fig. 1). The granite is Devonian in age (Dunning *et al.* 1990) and was deformed by a single episode of ductile deformation along its southeastern margin before deposition of a Carboniferous conglomerate (see Barr & Raeside 1989, Lin & Williams 1990 for the geological setting and the structural evolution of the shear zone).

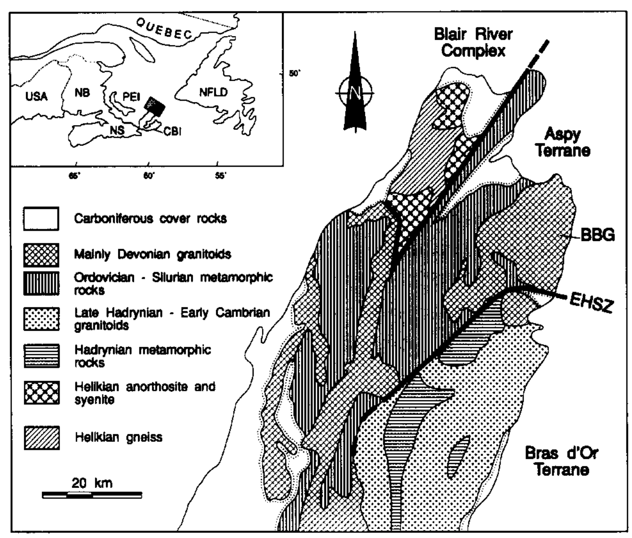

Fig. 1. Simplified geological map of northern Cape Breton Island (CBI) (adapted from Barr *et al.* 1989), showing geological setting of the Eastern Highlands shear zone (EHSZ) and Black Brook granite (BBG).

STRUCTURES DEVELOPED IN THE *S–C* MYLONITE

The Black Brook granite is medium-grained and largely composed of quartz, feldspar and a small amount of muscovite and biotite. Away from the shear zone, the granite is isotropic and undeformed. In the shear zone, the granite is strongly deformed with the development of an *S–C* fabric and a stretching lineation defined by elongate augen (Fig. 2a). Biotite is partially altered to chlorite.

On surfaces cut parallel to the stretching lineation (and the striae described below) and perpendicular to the *C*-surface, the *S–C* structure is well defined (Figs. 2b & c). *C*-surfaces are approximately planar. *S*-surfaces curve asymptotically into the *C*-surfaces, and in the ductilely, more strongly deformed rocks, the *C*-surfaces are more continuous and the overall angle between *S* and *C* is smaller.

On the microscopic scale, *C*-surfaces are discrete narrow zones (*C*-zones) defined by strongly deformed minerals. In these zones, quartz is completely dynamically recrystallized, forming an oblique shape fabric approximately parallel to the overall *S*-surface. Mica is strongly deformed and fine-grained, and is concentrated in narrow layers in the *C*-zones (Figs. 3a & b). Burg & Ponce de Leon (1985) described similar mica layers as the product of pressure-solution, but many of the mica layers described here are clearly the comminuted trails of mica fish, as described by Lister & Snoke (1984). The *S*-surface is a more penetrative foliation defined by the dimensional preferred orientation of arrays of less deformed mica crystals (Fig. 3a), mica fish (Fig. 3b), and locally by elongate and slightly recrystallized quartz between only slightly deformed feldspar crystals. In very strongly deformed granite the overall structure is similar, but all quartz is recrystallized and feldspar crystals are round with pressure shadows on both sides forming microscopic augen structures.

On surfaces cut perpendicular to the *C*-surface and parallel to the intersection of *C* and *S* (i.e. perpendicular to the striae described below), there is generally no clear mesoscopic difference between *S*- and *C*-surfaces; both curve between porphyroclasts, giving an integrated anastomosing fabric. Locally, *C*-surfaces can be recognized in hand specimen by their discreteness and continuity (Fig. 2d). In thin section, *C*-surfaces may be more easily recognized by their discrete, fine-grained zonal nature; however, the distinction between *S*- and *C*-surfaces may still be ambiguous. *C*-surfaces anastomose between porphyroclasts as do *S*-surfaces and are much less planar than they appear on the sections parallel to the stretching lineation and perpendicular to the *C*-surface (Fig. 3c). The local *C*-surface orientation commonly deviates considerably from the overall orientation. Similar mica layers to those described above are also developed (Fig. 3d).

Microfractures are observed in thin section along some *C*-surfaces but they are rare and not a characteristic feature. There is no evidence to suggest that they played a role in the development of the *C*-surfaces, but rather that they simply reflect an inherent weakness that localizes younger fractures in those surfaces. Evidence that they are not related to the formation of the *S–C* fabric is as follows: (1) the microfractures are only very locally developed and isolated, with individual fractures rarely more than a few millimeters long. They are short relative to the C-zones in which they occur; (2) the position of the fracture surfaces is strictly controlled by the weaker mica-rich *C*-surfaces; (3) when the rock is parted along the *C*-surfaces, the exposed surfaces (slickensides) are essentially the same no matter whether there were microfractures along the *C*-surfaces before parting or not. The only noticeable difference is that the *C*-surfaces with fractures are rusty rather than fresh.

The *C*-surfaces are weak surfaces along which the rock parts easily to form the observed slickensides, but there is no evidence that they were fractures during deformation as is usually implied by the term slickenside. The parting process is non-tectonic; it can occur during erosion (e.g. by the agency of flowing water, Fig. 2e) or can be developed manually (e.g. with a hammer and chisel, Fig. 2a). The surfaces exposed by parting in this way are mostly coated by thin films of very fine-grained mica and other material and have a shiny slickensided appearance. 'Ridge-in-groove'-type striae (Means 1987) are well developed (Figs 2d & e) and are parallel to the orthogonal projection of the stretching lineation on the *C*-surface. Individual grooves (or ridges), as visible in hand specimen, are a few millimeters wide and from less than 1 cm up to several centimeters long. The depth of the grooves (or the height of the ridges) is usually less than 1 mm. Locally, the structure is composite with the fine grooves and ridges combining to form coarser grooves and ridges (Figs. 2a & d). The morphology of the striae varies with differences in the microstructure of the host rock. In going from relatively undeformed coarse-grained mylonite to more strongly deformed fine-grained mylonite, both foliation and lineation become stronger, whereas slickenside grooves and ridges become progressively longer and shallower. If a specimen is broken cleanly into two pieces, the nesting of the ridges of either wall into the grooves of the other can be easily demonstrated using the 'book-opening-like' method described by Means (1987) (Fig. 3f). Approximately perpendicular to the striae are steps of both congruous and incongruous types (Figs. 2a & e). Incongruous steps are smooth and usually coated with mica (Figs. 2c and 3g). Congruous steps are rough and not coated with mica (Figs. 2b and 3h), and can be divided into two distinct groups according to the height of the risers. First-order congruous steps may be up to 1 cm high, whereas second-order congruous steps are usually less than 2 mm high. Laterally (relative to the direction of the striae), the size of the steps gradually diminishes. All this shows that the parting surfaces have the characteristics of classic slickensides, although they are penetrative.

INTERPRETATION

S–C structure has been studied in detail (e.g. Berthé *et al.* 1979, Lister & Snoke 1984), and it has been demonstrated that *S*-surfaces are related to the accumulation of finite strain and *C*-surfaces to zones of localized intense shear strain. However, previous studies have been mainly two dimensional and have only described and interpreted the two-dimensional geometry of the *S–C* microstructure as seen on the surfaces cut perpendicular to the intersection of the *S*- and *C*-surfaces. Striation on *C*-surfaces have been reported in ductilely deformed granite (e.g Berthé *et al.* 1979, Burg & Ponce de Leon 1985, Burg & Wilson 1988) but not described in detail, nor reported as the 'ridge-in-groove' type.

The 'ridge-in-groove'-type slickenside striation was first recognized by Means (1987) in both experimentally and naturally produced slickensides, but he offered no explanation for its formation. Will & Wilson (1989) also produced the 'ridge-in-groove'-type slickenside striation

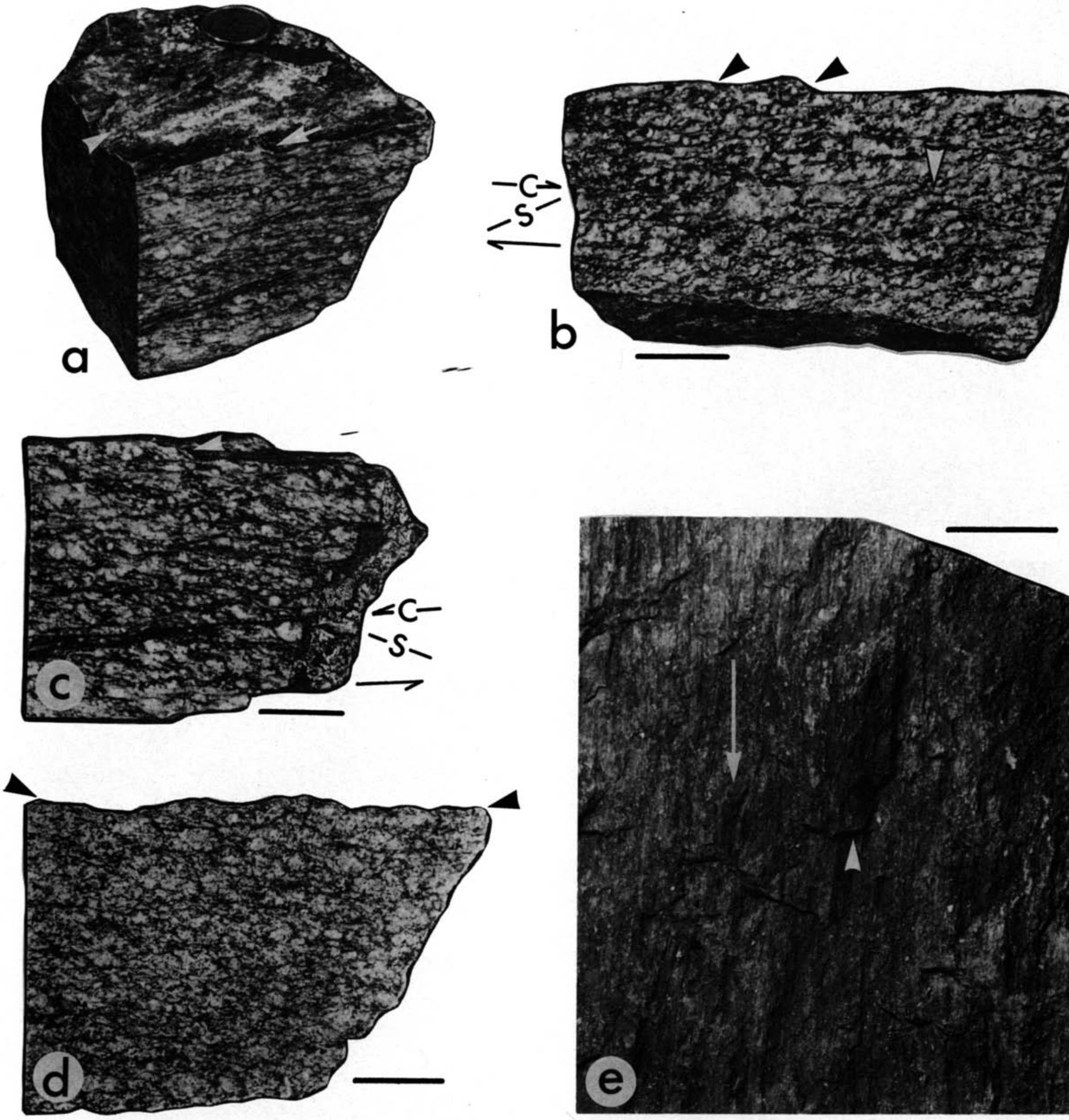

Fig. 2. Hand specimen photographs. (a) Three-dimensional view of an *S–C* mylonite. Top surface is a slickenside exposed by parting mainly along a *C*-surface. Shorter white arrow indicates a congruous step. Longer white arrow indicates an incongruous step. (b) & (c) Views of surfaces parallel to the striation and perpendicular to slickenside surface. Congruous steps in (b) indicated by black arrows; end of *C*-surface on the right indicated by white arrow. Incongruous step in (c) indicated by white arrow. (d) View of surface perpendicular to the striation. Trace of the slickenside and ridges and grooves in (e) indicated by black arrows. (e) A slickenside exposed mainly by parting along a *C*-surface. Longer white arrow is parallel to the striation and points in direction of movement of the missing wall. Shorter white arrow indicates a congruous step. The profile of this slickenside is shown in (d). Illumination is from top of photograph. All scale bars 2 cm.

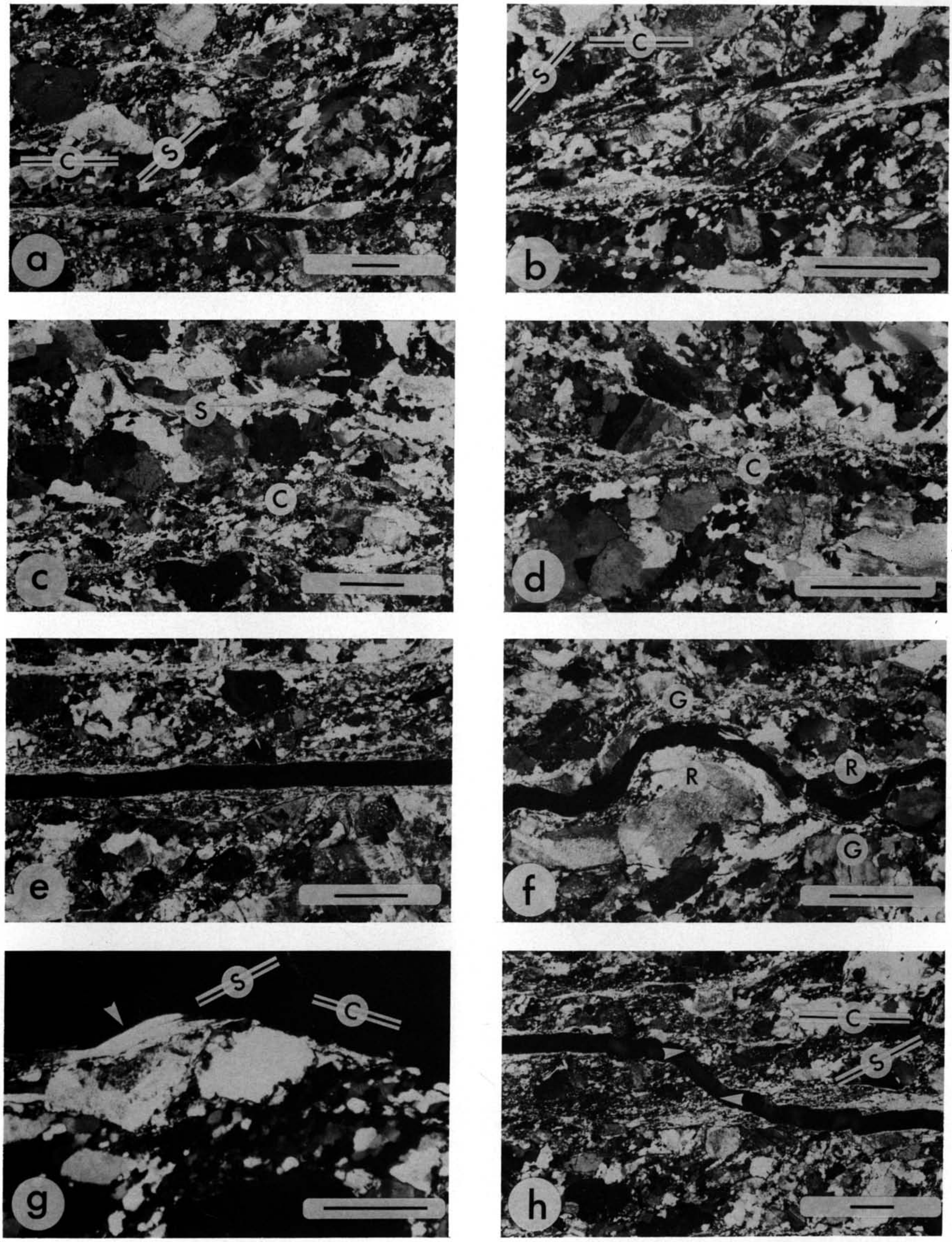

Fig. 3. Photomicrographs. (a) & (b) Sections parallel to lineation and perpendicular to the slickenside. *C*-surfaces are planar and are easily distinguished from *S*-surfaces. (c) & (d) Sections perpendicular to the striation. Difference between *S*- and *C*-surfaces is less clear than in (a) & (b), and *C*-surfaces are much less planar. Note mica concentration along *C*-surface in (d). (e) Section parallel to striation and perpendicular to the slickenside. Trace of parted surface (slickenside) is straight. (f) Section perpendicular to the striation. Trace of parted surface (slickenside) outlines the ridge-in-groove structure. Note perfect nesting of ridges (R) and grooves (G). The position of parting is controlled by the mica-rich zones in both (e) and (f). (g) Section parallel to striation and perpendicular to the slickenside. The parting stair-steps along a mica-fish from one *C*-surface to the next, to form the incongruous step indicated by white arrow. (h) Same orientation as (g). Breaking across the *S*-surfaces from one *C*-surface to another results in the congruous steps indicated by white arrows. Black areas between the two walls in (e), (f) & (h) and above the parting surface in (g), are epoxy-resin. All photographs taken with crossed polarizers. Scale bars 0.3 mm for (g), and 1.0 mm for (a)–(f) and (h).

experimentally. In their experiments, the deformation was first accommodated by the development of shear bands (C'). With increasing deformation, the shear bands linked up to form throughgoing shear planes (C). Will & Wilson (1989) suggested that the formation of the ridges and grooves was due to the change in the orientation of layer silicate (0001) planes, but they did not explain how this change was effected. In the mylonite described here, no shear bands are observed and if they were present as an intermediate step in the formation of the C-surfaces they have been obliterated.

Although approximately planar at the mesoscale the striated C-surfaces described by other workers and by ourselves are clearly corrugated at the microscopic scale (Fig. 4). It is this geometry that we wish to explain.

Two facts are crucial to the interpretation of the S–C structure. (1) The bulk deformation that formed the S–C mylonite was ductile. The confining pressure was sufficient to inhibit any deformation mechanism involving significant volume increase. (2) Grain scale deformation was not homogeneous. We assume that grain boundaries were weaker than the grains themselves and mica and quartz were weaker than feldspar. Feldspar shows little evidence of ductile deformation. Under these conditions, the imposed strain would be preferentially accommodated by movement along grain boundaries and by intracrystalline deformation of the mica and quartz. Given that for shear zone deformation the most efficient mechanism is that afforded by a planar anisotropy parallel to the shear zone boundary (viz. C-surfaces) (e.g. Price & Torok 1989), it is to be expected that fortuitous alignments of weak domains, such as suitably oriented long grain boundaries or mica grains, would tend to be linked and exploited as intergranular ductile shear zones. To be effective in a situation where volume increase is inhibited such shear zones would have to be planar or curvi-planar, with the axis of curvature parallel to the movement direction. Our assumption of the relative strengths of the grains requires that the micro-shear zones do not pass through the feldspar grains, but the feldspar is too abundant and uniform in distribution to allow the development of planar shear zones. However, the observed corrugated surfaces are a good approximation of a curvi-plane and we suggest that they represent optimization of the conditions such that the material deformed by ductilely accommodated slip on weak curvi-planar surfaces. During development of the C-zones, there was presumably significant grain boundary sliding, which can be considered a brittle process, but such C-zones were a product of true ductile deformation, in the normal usage of the term, in that on the scale of the zone there was no persistent loss of continuity. The rock breaks preferentially along the C-zones because of the mica concentrations in them, and not because of any fractures associated with their formation.

According to this interpretation, the size of the grooves and ridges should be related to the size of the strong grains. There is such a correlation in the material described here, in that the grooves are shallower in the finer grained mylonites. They are also of longer aspect ratio, but that can be explained in terms of higher strain. We suggest that the finer grained mylonites are more strongly deformed and that during deformation, stream-

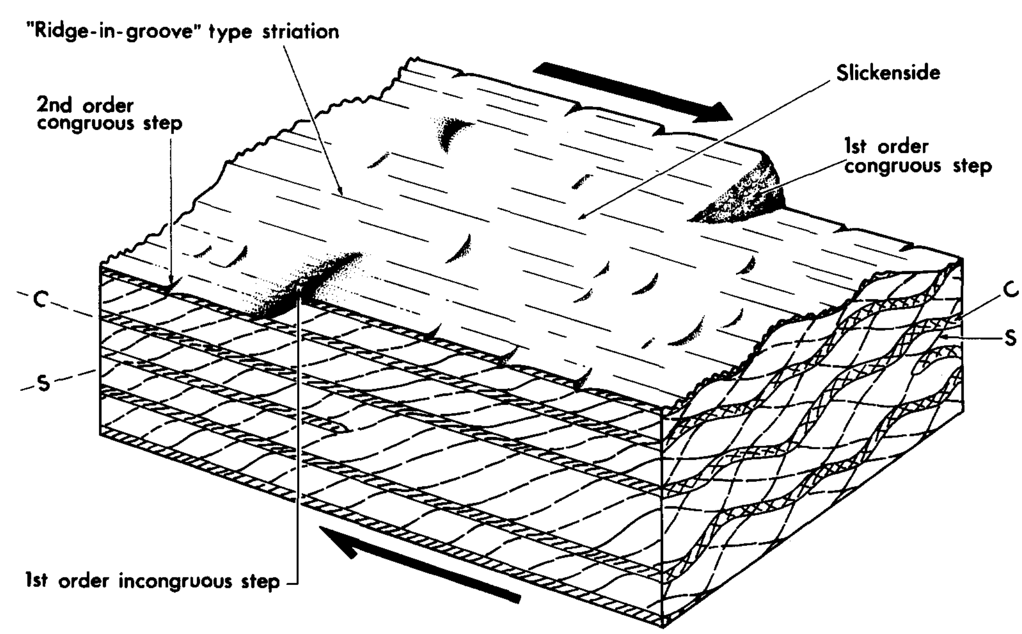

Fig. 4. Diagram showing relationship among slickensides, slickenside striations, slickenside steps and the S–C structure.

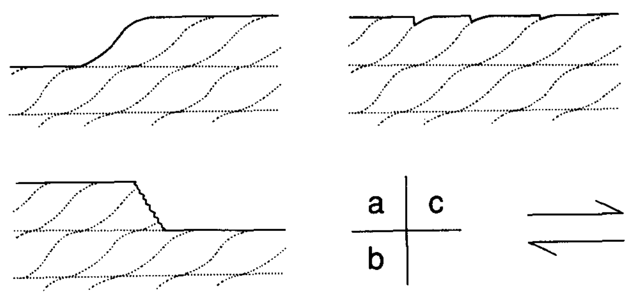

Fig. 5. Diagrammatic representation of the slickenside steps associated with *S–C* structure: (a) an incongruous step; (b) a first-order congruous step; (c) second-order congruous steps.

lining of the *C*-surfaces around the grains improves and the corrugations therefore become more cylindrical and the grooves thus longer in aspect ratio. The grain size correlation is further supported by comparison of the slickensides described here with those produced experimentally by Will & Wilson (1989). The material that they used (pyrophyllitic clay) is much finer (grain size = 10–50 μm) than the granite described here and the grooves and ridges that they produced are much finer, too (width = several tens of μm).

It follows from the above that the slickensides are surfaces that were exposed recently by parting parallel to weak *C*-surfaces developed in the rock during ductile flow. Similarly the ridge-in-groove striations represent corrugations in the ductilely formed *C*-surfaces (Fig. 4).

Many mechanisms have been proposed for the formation of slickenside steps. Steps formed by different mechanisms may face in different directions with respect to the shear sense, i.e. they may be congruous or incongruous (e.g. Paterson 1958, Tjia 1964, Norris & Barron 1968, Petit 1987). To the best of our knowledge, no slickenside steps developed in natural ductile shear zones have previously been reported.

The slickenside steps described here are both congruous and incongruous. Detailed examination, especially of sections parallel to the striae and perpendicular to the slickensides, shows that incongruous steps are the result of parting along *S*-surfaces (Figs. 2c, 3g and 5a) and first-order congruous steps are the result of breaking across *S*-surfaces during parting along adjacent *C*-surfaces (Figs. 2b, 3h and 5b). Second-order congruous steps form by breaking off the tips of the dihedra between *S*- and *C*-surfaces after parting along *C*-surfaces (Fig. 5c).

DISCUSSION

Curvi-planar shear surfaces

Our study shows that, in three dimensions, *C*-surfaces are not necessarily planar, but may be approximately curvi-planar with the linear generator parallel to the movement direction. This shear surface configuration is the result of minimizing the work done by taking maximum advantage of existing weaknesses, and may be more common than generally believed. It is possible that the process is also important at larger scales because natural rocks are rarely homogeneous and at whatever scale shear zones form they can be expected to exploit existing weaknesses. This may explain for example why some shear zones appear folded about their stretching lineations (e.g. Piasecki 1988).

Slickensides as ductile structures

The slickensides and striae described here have the appearance of typical traditional slickensides but whereas the latter are generally associated with a single surface that existed as a fracture during deformation, those described here are mimicking a penetrative ductile fabric. Consequently there is the potential for the rock to split along many closely spaced surfaces. We believe that as conditions become progressively more ductile there is a gradual transition from single slickenside surfaces through multiple surfaces of brittle origin (e.g. Hobbs *et al.* 1976, pp. 268–270) to the ductile structure described here.

Contrary to the common assumption that 'slickensides' are a brittle feature, we suggest that structures like those described here still be called slickensides for the following reasons: (1) the term 'slickenside' was originally a descriptive field term (Conybeare & Phillips 1822, Chamberlin & Challinor 1909, see Dennis 1967); (2) the brittle and ductile deformation is transitional, and the slickensides described here cannot be readily distinguished from those formed by brittle processes; (3) of existing terms only 'slickenside' fully describes the present structure; (4) the structures described here have already been called slickensides and slickenside striae with or without realizing that they are associated with ductile processes (Berthé *et al.* 1979, Burg & Ponce de Leon 1985, Burg & Wilson 1988, Waldron 1990 personal communication).

'Smoothness–roughness' technique for determining sense of shear

Most, if not all, mylonites are formed by non-coaxial laminar flow (see discussion by Lister & Snoke 1984) and *S–C* structures are usually developed to some degree. However, the latter are not always recognizable in the field, especially where the deformation is very strong and the angle between *S*- and *C*-surfaces is very small. In this case, if the rock can be parted along *C*-surfaces, as is usually the case where there are layer-silicates in the rock, the step structure described in this paper may prove to be very useful in helping determine the sense of shear in the field. Congruous steps can usually be easily recognized by their roughness, although incongruous steps may be too gentle and too smooth to be recognized where the angle between *S*- and *C*-surfaces is very small. The 'smoothness–roughness' technique of determining the sense of shear described by Billings (1954, pp. 149–150) may be valid in this case, even though both congruous and incongruous steps are present.

In using this technique, one should make sure that the steps are not the result of tectonic fracturing associated with later brittle deformation, and that the structure developed is the *S–C* structure, not the *C–C′* structure as experimentally produced by Will & Wilson (1989). Tectonic fractures are not only restricted to the slickenside surface; they are expected to persist into the rock on either side of the slickensides (e.g. Petit 1987). Pure *C–C′* structure without *S*-surfaces are rare and, usually, shear bands (*C′*) cannot be confused with *S*-surfaces in the field (Platt & Vissers 1980, White *et al.* 1980).

Acknowledgements—We are grateful to Drs Laurel Goodwin, Steve Ralser, John Spray and Joe White for stimulating discussion and comments and to Angel Gomez, Bob McCulloch and Ansel Murphy for assistance with figure and thin section preparation. The work was supported by NSERC operating grant OGP007419 to P. F. Williams and the paper forms part of S. Lin's Ph.D. thesis at the University of New Brunswick.

REFERENCES

Barr, S. M. & Raeside, R. P. 1989. Tectono-stratigraphic terranes in Cape Breton Island, Nova Scotia: Implications for the configuration of the northern Appalachian orogen. *Geology* **17**, 822–825.

Bates, R. L. & Jackson, J. A. (editors). 1987. *Glossary of Geology* (3rd edn). American Geological Institute.

Berthé, D., Choukroune, P. & Jegouzo, P. 1979. Orthogneiss, mylonite and non coaxial deformation of granite: the example of the South Armorican shear zone. *J. Struct. Geol.* **1**, 31–42.

Billings, M. P. 1954. *Structural Geology* (2nd edn). Prentice-Hall, Englewood Cliffs, New Jersey.

Burg, J. P. & Ponce de Leon, M. I. 1985. Pressure-solution structures in a granite. *J. Struct. Geol.* **7**, 431–436.

Burg, J. P. & Wilson, C. J. L. 1988. A kinematic analysis of the southernmost part of the Bega Batholith. *Aust. J. Earth Sci.* **35**, 1–13.

Dennis, J. G. (editor). 1967. *International Tectonic Dictionary: English terminology*. American Association of Petroleum Geologists.

Dunning, G. R., Barr, S. M., Raeside, R. P. & Jamieson, R. A. 1990. U–Pb zircon, titanite, and monazite ages in the Bras d'Or and Aspy terranes of Cape Breton Island Nova Scotia: Implications for igneous and metamorphic history. *Bull. geol. Soc. Am.* **102**, 322–330.

Fleuty, M. J. 1975. Slickensides and slickenlines. *Geol. Mag.* **112**, 319–322.

Hobbs, B. E., Means, W. D. & Williams, P. F. 1976. *An Outline of Structural Geology*. Wiley, New York.

Lin, S. & Williams, P. F. 1990. The structural evolution of the Eastern Highlands shear zone in Cape Breton Island, Nova Scotia (abs.). *Nova Scotia Dept. Mines and Energy Rep.* **90-3**, 42.

Lister, G. S. & Snoke, A. W. 1984. *S–C* mylonites. *J. Struct. Geol.* **6**, 617–638.

Means, W. D. 1987. A newly recognized type of slickenside striation. *J. Struct. Geol.* **9**, 585–590.

Norris, D. K. & Barron, K. 1968. Structural analysis of features on natural and artificial faults. In: *Research in Tectonics* (edited by Baer, A. J. & Norris, D. K.). *Geol. Surv. Pap. Can.* **68-52**, 136–167.

Paterson, M. S. 1958. Experimental deformation and faulting in Wombeyan marble. *Bull. geol. Soc. Am.* **69**, 465–476.

Petit, J. P. 1987. Criteria for the sense of movement on fault surfaces in brittle rocks. *J. Struct. Geol.* **9**, 597–608.

Piasecki, M. A. J. 1988. A major ductile shear zone in the Bay d'Espoir area, Gander terrane, southeastern Newfoundland. *Curr. Res. Newfoundland Dept Mines Rep.* **88–1**, 135–144.

Platt, J. P. & Vissers, R. L. M. 1980. Extensional structures in anisotropic rocks. *J. Struct. Geol.* **2**, 397–410.

Price, G. P. & Torok, P. A. 1989. A new simple shear deformation apparatus for rocks and soils. *Tectonophysics* **158**, 291–309.

Tjia, H. D. 1964. Slickensides and fault movements. *Bull. geol. Soc. Am.* **75**, 683–686.

White, S. H., Burrows, S. E., Carreras, J., Shaw, N. D. & Humphreys, F. J. 1980. On mylonites in ductile shear zones. *J. Struct. Geol.* **2**, 175–187.

Will, T. M. & Wilson, C. J. L. 1989. Experimentally produced slickenside lineations in pyrophyllitic clay. *J. Struct. Geol.* **11**, 657–667.